Spectral properties and energy transfer in Er^{3+}/Yb^{3+} co-doped $LiYF_4$ crystal*

WANG Pei-yuan (汪沛渊)[1], **XIA Hai-ping** (夏海平)[1]**, **PENG Jiang-tao** (彭江涛)[1], **HU Hao-yang** (胡皓阳)[1], **TANG Lei** (唐磊)[1], **ZHANG Yue-pin** (张约品)[1], **CHEN Bao-jiu** (陈宝玖)[2], and **JIANG Hao-chuan** (江浩川)[3]

1. Key Laboratory of Photoelectronic Materials, Ningbo University, Ningbo 315211, China

2. Department of Physics, Dalian Maritime University, Dalian 116026, China

3. Ningbo Institute of Materials Technology and Engineering, Chinese Academy of Sciences, Ningbo 315211, China

(Received 1 March 2013)

©Tianjin University of Technology and Springer-Verlag Berlin Heidelberg 2013

Laser crystals of $LiYF_4$ (LYF) singly doped with Er^{3+} in 2.0% and co-doped with Er^{3+}/Yb^{3+} in about 2.0%/1.0% molar fraction in the raw composition are grown by a vertical Bridgman method. X-ray diffraction (XRD), absorption spectra, fluorescence spectra and decay curves are measured to investigate the structural and luminescent properties of the crystals. Compared with the Er^{3+} singly doped sample, obviously enhanced emission at 1.5 μm wavelength and green and red up-conversion emissions from Er^{3+}/Yb^{3+} co-doped crystal are observed under the excitation of 980 nm laser diode. Meanwhile, the emission at 2.7 μm wavelength from Er^{3+} singly doped crystal is reduced. The fluorescence decay time ranging from 18.60 ms for Er^{3+} singly doped crystal to 23.01 ms for Er^{3+}/Yb^{3+} co-doped crystal depends on the ionic concentration. The luminescent mechanisms for the Er^{3+}/Yb^{3+} co-doped crystals are analyzed, and the possible energy transfer processes from Yb^{3+} to Er^{3+} are proposed.

Document code: A **Article ID:** 1673-1905(2013)04-0285-4

DOI 10.1007/s11801-013-3034-2

The host crystal $LiYF_4$ is very suitable for the incorporation with trivalent rare-earth ions, in which the Y^{3+} ions are substituted[1], and it is also extremely suitable for the host of mid-infrared (IR) solid state lasers due to the significantly low phonon energy and wide optical transmittance from 200 nm to 5 μm. Moreover, the fluorides have the longer lifetime of the excited electronic states in these systems compared with that in traditional oxide systems when they are used as a laser host. Although much attention has been paid to the near IR and mid-IR optical emission of Er^{3+}/Yb^{3+} doped glasses and crystals[2-5], there has been rare study on that in Er^{3+}/Yb^{3+} co-doped $LiYF_4$ crystal. It is proposed that the relatively homogeneous concentrations of Er^{3+} and Yb^{3+} in $LiYF_4$ crystal can be obtained due to the distribution coefficients of both Er^{3+} and Yb^{3+} in $LiYF_4$ crystals are close to 1[6], which is extremely important for the practical application in laser device.

In this paper, Er^{3+}/Yb^{3+} co-doped $LiYF_4$ crystal as well as Er^{3+} singly-doped $LiYF_4$ crystal are grown by Bridgman method, and Yb^{3+} is introduced into $LiYF_4$ crystal as the sensitizer to increase the pump efficiency of 980 nm laser diode. The optical emissions of the obtained crystal from visible to mid-IR wavelength are studied systematically to understand the energy transfer processes between Yb^{3+} and Er^{3+}.

The Bridgman technique is used to grow the Er^{3+}/Yb^{3+} co-doped $YLiF_4$ crystal. The detailed process for crystal growth was described in Refs.[7-10]. The molar composition of the powder is $51.5LiF\text{-}(48.5\text{-}2\text{-}x)YF_3\text{-}2ErF_3\text{-}xYbF_3$ (x=0 or 1). The four mixtures were ground for 1 h in a mortar. In order to synthesize anhydrous Er^{3+}/Yb^{3+} co-doped $LiYF_4$ polycrystalline materials, the fluoride powder was treated with anhydrous HF at 750–800 ℃ for 8–10 h to ensure the complete removal of residual moisture in the fluorides.

The grown crystals by the Bridgman method are about 105 mm in length and 10 mm in diameter. They are pink and transparent. The as-grown crystals were cut into small pieces and well polished by CeO_2 powder on both sides to about 2.5 mm-thickness for optical measurements. Structures of the samples were investigated by X-ray diffraction (XRD) using an XD-98X diffractometer (XD-3, Beijing). The absorption spectra were measured using a U-4100UV/VIS/NIR spectrophotometer in a range from 300 nm to 1750 nm. The emission spectra were recorded by a Triax 320 type spectrometer in a wavelength region of 400–3000 nm excited by 980 nm.

* This work has been supported by the National Natural Science Foundation of China (Nos.51272109，50972061 and 61078061), the Natural Science Foundation of Zhejiang Province (No.R4100364), the Natural Science Foundation of Ningbo City (No.2012A610115), and the K. C. Wong Magna Fund in Ningbo University.

** E-mail: xiahaiping@nbu.edu.cn

The fluorescence lifetime was tested by the FLSP920 fluorescence spectrophotometer. Meanwhile, the concentrations of Er^{3+}/Yb^{3+} ions in the Er^{3+}/Yb^{3+} co-doped $LiYF_4$ single crystals were measured by inductively coupled plasma atomic emission spectroscopy (ICP-AES, PerkinElmer Inc., Optima 3000). All the measurements were performed at room temperature.

In order to identify the chemical phase, the powder XRD measurements of Er^{3+}/Yb^{3+} co-doped $LiYF_4$ crystals are performed. The result of powder XRD is shown in Fig.1, and the diffraction peaks are assigned. The XRD spectrum shows that the diffraction peaks and relative intensity of the crystal sample are very similar to those of JCPD 77-0816 $LiYF_4$. Therefore, the crystal belongs to a tetragonal phase with a space group of I41/a, and the current doping level does not cause any obvious peak shift or second phase.

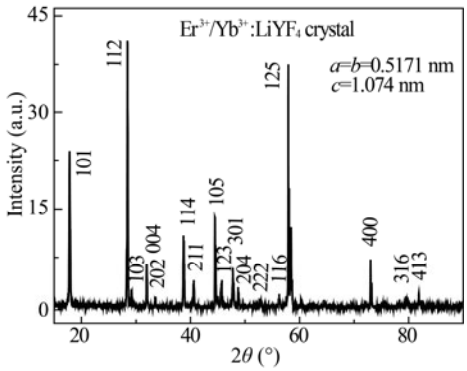

Fig.1 Powder XRD pattern of Er^{3+}/Yb^{3+} co-doped crystal with *a*=*b*=0.5171 nm and *c*=1.074 nm

In Fig.2, the most significant difference is the absorption band at ~958 nm which is broader and more intense in the Er^{3+}/Yb^{3+} co-doped sample. All absorption bands of Er^{3+}:$LiYF_4$ phosphor can be assigned to 4f-transitions of the Er^{3+} ion. The peaks with maximum at ~361 nm, ~376 nm, ~407 nm, ~448 nm, ~484 nm, ~519 nm, ~540 nm, ~650 nm, ~799 nm, ~958 nm and ~1494 nm correspond to the $^4I_{15/2} \rightarrow {}^4G_{9/2}$, $^4I_{15/2} \rightarrow {}^4G_{11/2}$, $^4I_{15/2} \rightarrow {}^2H_{9/2}$, $^4I_{15/2} \rightarrow {}^4F_{5/2}$, $^4I_{15/2} \rightarrow {}^4F_{7/2}$, $^4I_{15/2} \rightarrow {}^2H_{11/2}$, $^4I_{15/2} \rightarrow {}^4S_{3/2}$, $^4I_{15/2} \rightarrow {}^4F_{9/2}$, $^4I_{15/2} \rightarrow {}^4I_{9/2}$, $^4I_{15/2} \rightarrow {}^4I_{11/2}$ and $^4I_{15/2} \rightarrow {}^4I_{13/2}$ transitions of Er^{3+} ion, respectively. The broadening of the absorption band near 958 nm in Er^{3+}/Yb^{3+} co-doped $LiYF_4$ is caused by the $^2F_{7/2} \rightarrow {}^2F_{5/2}$ transition of the Yb^{3+} ions, which is not present in the Er^{3+} singly doped $LiYF_4$ crystal.

The concentrations of Er^{3+} and Yb^{3+} ions in the co-doped crystals are listed in Tab.1. From Fig.2, we can clearly know that the absorption coefficient of the top section of the crystal A is less than that of the bottom section of the crystal B. This indicates that the concentrations of Er^{3+} and Yb^{3+} in the top section are lower than those in the bottom. In other words, the concentrations of Er^{3+} and Yb^{3+} decrease along the crystal growth direction, which implies that the effective segregation coefficient of Er^{3+} and Yb^{3+} is higher than 1 in the $LiYF_4$ crystal, which is consistent with the results of other reports[6].

In the measurements of emission spectra, the same experimental conditions for both Er^{3+} doped and Er^{3+}/Yb^{3+} co-doped samples are maintained in order to get the comparable results. Compared with Yb^{3+}-free sample, it is found from Fig.3 that the emission intensity at 2.7 μm from the excited $^4I_{11/2}$ state is reduced when Yb^{3+} is introduced into Er^{3+}:$LiYF_4$ crystal. For all Er^{3+}/Yb^{3+} co-doped $LiYF_4$ single crystals, the emissions at ~2.7 μm show sharp bands, while for Er^{3+}/Yb^{3+} glasses, they are inhomogeneously broadened due to the glass matrix[2], which is not beneficial to the laser output.

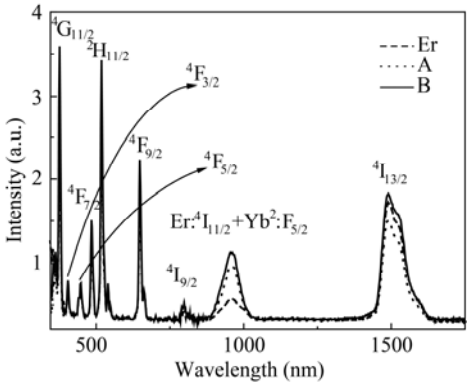

Fig.2 Absorption spectra of Er^{3+} doped and Er^{3+}/Yb^{3+} co-doped $YLiF_4$ single crystals

Tab.1 Concentrations of Er^{3+} ions and Yb^{3+} ions with unit of molar fraction in the crystals

Sample (No.)	A (%)	B (%)	Er (%)
Er^{3+}	1.96	2.06	2.02
Yb^{3+}	0.99	1.02	0.00

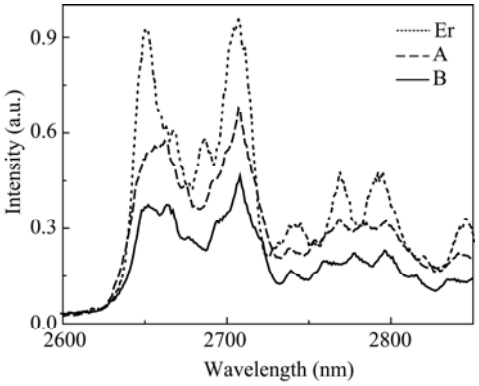

Fig.3 Emission spectra of Er^{3+}/ Yb^{3+} co-doped and Er^{3+} singly doped $LiYF_4$ crystals under 980 nm excitation

The emission spectra in Fig.4(a) consist of the characteristic bands centrically peaked at 1.53 μm originating from the $^4I_{13/2}$ to the terminal $^4I_{15/2}$ level, and in Fig.4(b) the peaks at 0.52 μm, 0.55 μm and 0.66 μm result from the $^2H_{11/2}$, $^2S_{3/2}$ and $^4F_{9/2}$ metastable levels to the $^4I_{15/2}$ level. Compared with Yb^{3+}-free sample, it is noted that both the emission and up-conversion emission intensities increase greatly when Yb^{3+} is introduced into Er^{3+}:$LiYF_4$

crystal. The similar enhanced phenomena were also observed in other Yb^{3+}/Er^{3+} co-doped matrices[11,12].

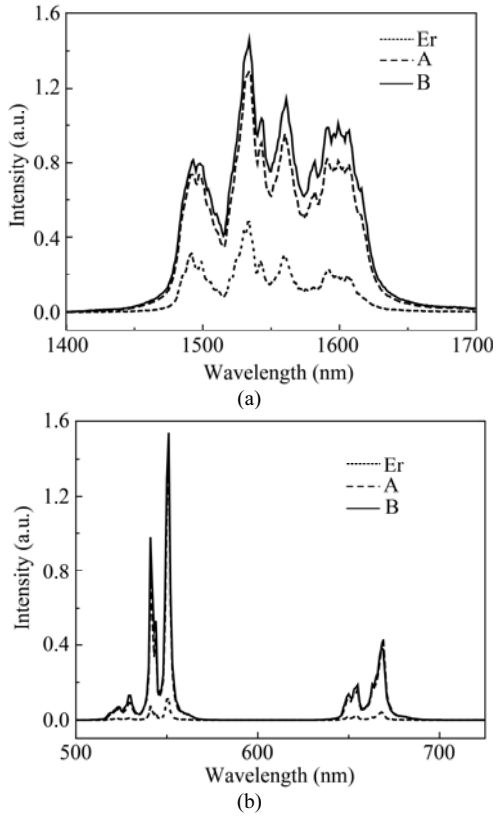

Fig.4 (a) Emission and (b) up-conversion emission spectra of Er^{3+}/ Yb^{3+} co-doped and Er^{3+} singly doped $LiYF_4$ crystals under 980 nm excitation

From Figs.3 and 4, we can also clearly know that the emission intensity of the bottom section of crystal (sample B) is slightly stronger than that of the top section (sample A). It is caused by the different doping concentrations of Yb^{3+} and Er^{3+} at the different crystal locations, which results from the effective segregation phenomena of the trivalent rare-earth ions in $LiYF_4$ crystal. The emission spectra are used to estimate all the stimulated emission parameters. The stimulated emission cross-sections $\sigma_{emi}(\lambda_p)$ for $^4I_{11/2}\rightarrow {}^4I_{13/2}$ and $^4I_{13/2}\rightarrow {}^4I_{15/2}$ transitions are evaluated from the measured emission line shape as[13]

$$\sigma_{emi}(\lambda_p)=\frac{\lambda_p^4 A}{8\pi c n^2 \Delta\lambda_{eff}}, \quad (1)$$

where λ_p is the peak fluorescence wavelength, $\Delta\lambda_{eff}$ is the effective line width of the transition, n is the refractive index of the host crystal, c is the velocity of light, and A is the radiative transition probability of the transition. Since the emission band is found to be slightly asymmetric, the effective line width $\Delta\lambda_{eff}$ is determined using the expression of $\Delta\lambda_{eff}=\int\frac{I(\lambda)}{I_p}d\lambda$, where I_p is the peak fluorescence intensity corresponding to λ_p. The stimulated emission cross-sections $\sigma_{emi}(\lambda_p)$ for 2.7 μm and 1.5 μm are calculated and listed in Tab.2.

Tab.2 Stimulated emission cross-sections $\sigma_{emi}(\lambda_p)$ for 2.7 μm and 1.5 μm

Sample	σ_{emi} (2.7) (cm^2)	σ_{emi} (1.5) (cm^2)
Er	10.11×10^{-20}	2.90×10^{-20}
A	5.38×10^{-20}	10.46×10^{-20}
B	8.16×10^{-20}	12.48×10^{-20}

The possible mechanisms of the energy transfer processes between Er^{3+} and Yb^{3+} ions have been reported by Vijay Singh et al[14]. Here we attempt to quantitatively investigate the energy transfers between Er^{3+} and Yb^{3+}. The energy level diagram for the Er^{3+}/Yb^{3+} co-doped $LiYF_4$ crystal is shown in Fig.5.

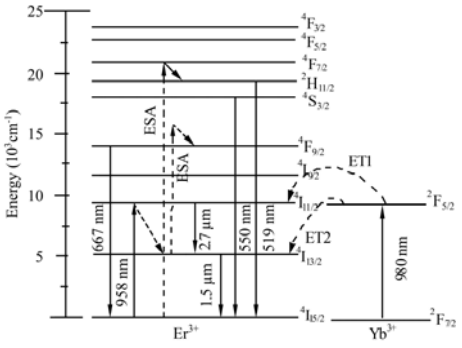

Fig.5 Energy level diagram of Er^{3+} and Yb^{3+}

When the Yb^{3+} is introduced, the pump light at 980 nm is mainly absorbed by Yb^{3+} via the transition $^2F_{7/2}\rightarrow {}^2F_{5/2}$. It should be noted that when co-doped samples are excited by high power continuous laser at 980 nm, the $^2F_{5/2}$ state can be highly populated, where the $^2F_{5/2}$ is a metastable state, and thus the energy transfer from Yb^{3+}:$^2F_{5/2}$ to Er^{3+}:$^4I_{11/2}$, $^4I_{13/2}$ can take place due to the good energy match. These energy transfer processes from Yb^{3+} to Er^{3+} can rapidly populate the Er^{3+}: $^4I_{13/2}$ and Er^{3+}: $^4I_{11/2}$ levels. As a consequence, a greatly enhanced emission at 1.5 μm from $^4I_{13/2}\rightarrow {}^4I_{15/2}$ transition can be observed. The energy transfer rate of Yb^{3+}:$^2F_{5/2}\rightarrow Er^{3+}$:$^4I_{13/2}$ (ET2) is demonstrated to be much smaller than that of Yb^{3+}:$^2F_{5/2}\rightarrow Er^{3+}$:$^4I_{11/2}$ (ET1) because the energy mismatch of Yb^{3+}:$^2F_{5/2}$ and Er^{3+}: $^4I_{13/2}$ is larger. The most likely up-conversion mechanisms are two successive ET1 processes in the Er^{3+}/Yb^{3+} co-doped samples[2]. The pump energy is efficiently absorbed by the Yb^{3+} ion in its ground state, which promotes these ions to their $^2F_{5/2}$ excited state. The excited Yb^{3+} ions transfer their energy to adjacent Er^{3+} ions in the $^4I_{15/2}$ ground state, and excite them to the $^4I_{11/2}$ state. Fast energy transfer from the second excited Yb^{3+} ion or direct absorption of the photon at 980 nm can further excite these Er^{3+} ions from the $^4I_{11/2}$ state to the $^4F_{7/2}$ level. Another possibility of populating the $^4F_{7/2}$ level is the interaction between two excited Er^{3+} ions followed by the energy transfer process in the $^4I_{11/2}$ state. After nonradiative relaxation from the $^4F_{7/2}$ level to the $^2H_{11/2}$ or $^4S_{3/2}$ level, the Er^{3+} ions can either return to the ground state, introducing the emission of green light, or further nonra-

diatively relax to the $^4F_{9/2}$ level, leading to the emission of red light. Since this $^4F_{7/2}$, $^4I_{11/2}\rightarrow{}^4F_{9/2}$, $^4F_{9/2}$ process involves two excited Er^{3+} ions, only the emission of red light is enhanced when the system is strongly pumped with 980 nm light. The latter is achieved more easily in the co-doped material due to its larger absorption cross section.

As shown in Fig.4, Yb^{3+} introduction promotes the green emission ($^2H_{11/2}/^4S_{3/2}\rightarrow{}^4I_{15/2}$), the red up-conversion emission ($^4F_{9/2}\rightarrow{}^4I_{15/2}$), and 1.5 μm down-conversion emission ($^4I_{13/2}\rightarrow{}^4I_{15/2}$) of Er^{3+}. It is proposed that the process of up-conversion emission depopulates the $^4I_{11/2}$ level, and the energy process of Yb^{3+}:$^2F_{5/2}\rightarrow Er^{3+}$:$^4I_{11/2}$ (ET2) populates the $^4I_{13/2}$ level, which is not beneficial to the emission at 2.7 μm (Er^{3+}: $^4I_{11/2}\rightarrow{}^4I_{13/2}$), and results in the reduction of the emission by introducing Yb^{3+}.

The fluorescent decays for $^4I_{13/2}\rightarrow{}^4I_{15/2}$ transition of Er^{3+} in Er^{3+} singly doped sample and Yb^{3+}/Er^{3+} co-doped samples under 980 nm are measured and shown in Fig.6. From the decay curves, the average fluorescent lifetime can be calculated by[15]:

$$\overline{\tau}=\frac{\int I(t)t\mathrm{d}t}{\int I(t)\mathrm{d}t}, \tag{2}$$

where $I(t)$ represents the luminescence intensity as a function of time t. The measured lifetime of Er^{3+}:$^4I_{13/2}$ is increased from 18.60 ms for the Er^{3+} singly doped $LiYF_4$ crystal to 23.01 ms and 20.80 ms for the upper part (A) and lower part (B) of Er^{3+}/Yb^{3+}co-doped samples, respectively, indicating that the Yb^{3+} introduction populates $^4I_{13/2}$ level of Er^{3+} greatly.

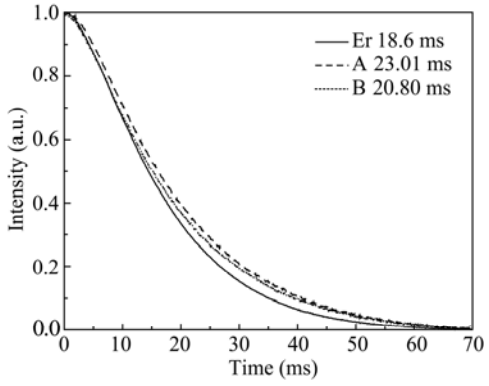

Fig.6 Decay curves of the Er^{3+}:$^4I_{13/2}$ level in $LiYF_4$ crystals doped with Er^{3+} and Er^{3+}/Yb^{3+} ions at 1.5 μm under 980 nm excitation

In summary, intense 1.5 μm and up-conversion emissions from Er^{3+}/Yb^{3+} co-doped $LiYF_4$ single crystal are observed, which are prepared by the Bridgman technique. Intense 1.5 μm and up-conversion emission is obtained due to the efficient energy transfer between Yb^{3+} and Er^{3+} ions. The maximum calculated emission cross sections at 1.5 μm and 2.7 μm wavelength of Er^{3+}/Yb^{3+} co-doped $LiYF_4$ crystal are 12.48×10^{-20} cm^2 and 8.16×10^{-20} cm^2, respectively. Introducing Yb^{3+} ion into the Er^{3+} doped $LiYF_4$ crystal can play a significant role to enhance the 1.5 μm and up-conversion emissions. So we can conclude that the Er^{3+}/Yb^{3+} co-doped $LiYF_4$ single crystal can be a promising material for the infrared laser.

References

[1] Chen H. B., Fan S. J., Xia H. P. and Xu J. Y., J. Mater. Sci. Lett. **21**, 457 (2002).

[2] De Sousa D. F., Zonetti L. F. C., Bell M. J. V., Lebullenger R. and Hernandes A. C., J. Appl. Phys. **85**, 2502 (1999).

[3] Gao S. X., Li X. Q. and Zhang S. M., Optik **121**, 2110 (2010).

[4] Li S. F., Zhang M., Peng Y., Zhang Q. Y. and Zhao M. S., J. Rare Earths **28**, 237 (2010).

[5] Zhong H. Y. and Cao W. H., J. Funct. Mater. **40**, 896 (2009).

[6] Namujilatu Y. B., Ruan Y. F. and Yuan J., Journal Chin. Ceram. Soc. **29**, 585 (2001).

[7] C. W. Lan, J. Cryst. Growth **229**, 595 (2001).

[8] Anandha Badu G., Subramaniyanraja R., Karunagaran N., Perumal Ramasamy R., Ramasamy P., Ganesamoorthy S. and Gupta P. K., J. Cryst. Growth **338**, 42 (2012).

[9] Campbell T. A. and Koster J. N., J. Cryst. Growth **147**, 408 (1995).

[10] Yu X. F., Chen H. B., Wang S. J., Zhou Y. F., Wu A. H. and Dai X. X., J. Inorg. Mater. **26**, 924 (2011).

[11] Huang J. H., Chen Y. J., Gong X. H., Lin Y. F., Luo Z. D. and Huang Y. D., Laser Phys. **22**, 146 (2012).

[12] Huang J. H., Chen Y. J., Gong X. H., Lin Y. F., Luo Z. D. and Huang Y. D., Appl. Phys. B **97**, 431 (2009).

[13] Philipps J. F., Topfer T., Ebendorff-Heidepriem H., Ehrt D. and Sauerbrey R., Appl. Phys. B **72**, 399 (2001).

[14] Vijay Singh, Vineet Kumar Rai and Markus Hearse, J. Appl. Phys. **112**, 063105 (2012).

[15] Murakami S., Herren M., Rau D. and Morita M., Chim. Acta **300**, 1014 (2000).